Mausam, (1986), **37**, 1, 55-60

551.558.21 : 551.511

Dynamic effects of orography on the large scale motion of the atmosphere — Zonal flow and elliptic barrier with maximum height of one km*

S. N. BAVADEKAR and R. M. KHALADKAR

Indian Institute of Tropical Meteorology, Pune

सार — वायुमंडल के बड़े पैमाने की गति पर पर्वतीय गतिक प्रभावों की अनुरूपता के लिए तीन स्तर के पूर्वग समीकरण निदर्श का विकास किया गया है। इस निदर्श के कार्य की जांच क्षेत्रीय पछुआ पवनों के प्रवाह तथा दीर्घवृत्ताकार रोधक, जिसकी अपने केन्द्र में अधिकतम ऊंचाई एक किलोमीटर है, के साथ परीक्षण करके की जाती है। इस निदर्श को 5 दिनों के लिए समाकलित किया गया है। पूर्वानुमान क्षेत्रों को प्रस्तुत किया गया है और उसके परिणामों पर विचार-विमर्श किया गया है।

ABSTRACT. The three level primitive equation model is being developed to simulate the dynamic effects of orography on the large scale motion of the atmosphere. The model performance is tested by conducting the experiment with zonal westerly flow and elliptic barrier with maximum height of one km at the centre of the region. The model is integrated for 5 days. The forecast fields are presented and the results are discussed.

1. Introduction

The multilevel primitive equation baroclinic model is being developed at the Forecasting Research Division of Indian Institute of Tropical Meteorology, Pune. Simplified version of the model was used by Singh and Saha (1976) and the computational stability of the finite difference schemes, was tested. The effects of friction, diabatic heating due to convection and sensible heating due to air-sea interaction were excluded in the model. The model also did not consider the forcing due to orography.

The present paper deals with the simulation of dynamic effects of orography assuming idealized wind and low type of orography as an obstacle to flow. The evolution of the flow is studied with the help of three level P.E. model in pressure coordinate. The work on similar type was also performed by Das and Bedi (1976) with the help of 3 level P.E. model in σ coordinate system and by using idealized wind and orography. They have, however, quoted about some difficulties regarding conversion of results from σ to p system, etc.

2. The model design

The model consists of following set of equations :

u and v momentum equations :

$$\frac{\partial u}{\partial t} + \frac{\partial}{\partial x}(uu) + \frac{\partial}{\partial y}(uv) + \frac{\partial}{\partial p}(u\omega) - fv + \frac{\partial \phi}{\partial x} = F_x \tag{1}$$

$$\frac{\partial v}{\partial t} + \frac{\partial}{\partial x}(vu) + \frac{\partial}{\partial y}(vv) + \frac{\partial}{\partial p}(v\omega) + fu + \frac{\partial \phi}{\partial y} = F_y \tag{2}$$

Equation of continuity :

$$\frac{\partial u}{\partial x} + \frac{\partial v}{\partial y} + \frac{\partial \omega}{\partial p} = 0 \tag{3}$$

Hydrostatic approximation :

$$\frac{\partial \phi}{\partial p} = -\frac{R'T}{p} \tag{4}$$

Thermal equation :

$$\frac{\partial}{\partial t}(c_p T) + \frac{\partial}{\partial x}(c_p T u) + \frac{\partial}{\partial y}(c_p T v) + \frac{\partial}{\partial p}(c_p T \omega) + \frac{\partial \phi}{\partial p}\omega = D_t \tag{5}$$

The dependent variables are u, v, ω, ϕ and T. The frictional and diffusion terms represented by F_x, F_y and D_t are dropped in the present experiment.

*The paper was presented in the symposium 'Indo-French School on recent advances in Computer Techniques in Meteorology, Biomechanics and Applied Systems' held at I.I.T., New Delhi, 4-13 February 1980.

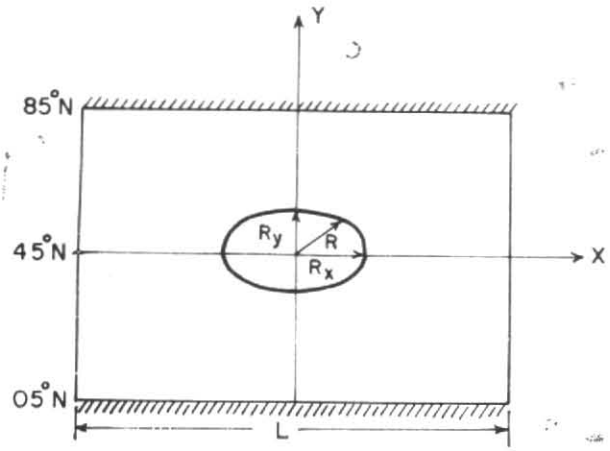

Fig. 1. The domain of limited area P.E. model. The orography is shown at the centre of the region

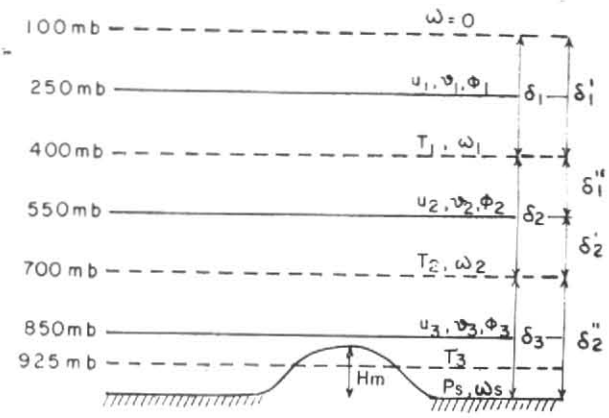

Fig. 2. Vertical structure of the three level P.E. model

The coriolis parameter f is allowed to vary in β plane by using the expression :

$$f = f_0 + \beta y \tag{6}$$

where, $f_0 = 10^{-4}$ sec^{-1} at 45°N and corresponding β value is 1.62×10^{-11} m^{-1} sec^{-1}.

2.1. *Boundary conditions*

$\omega = 0$ at 100 mb which is also the top level of the model atmosphere. The lower boundary condition can be obtained by using surface tendency equation :

$$\frac{\partial p_s}{\partial t} + u_s \frac{\partial p_s}{\partial x} + v_s \frac{\partial p_s}{\partial y} - \omega_s = 0 \tag{7}$$

The slipping walls are assumed at north and south boundaries of the domain of integration (*see* Fig. 1), whereas the cyclic boundary conditions are assumed in the east-west direction with the cycle of length L.

2.2. *The vertical structure of the model*

The numerical solution is obtained by integrating the model using three level structure (*see* Fig. 2).

The wind components u, v and the geopotential ϕ are specified on 250, 550, and 850 mb levels. The temperature T is specified on 400, 700 and 925 mb levels. The temperature at 925 mb is assumed to remain constant throughout the period of integration. The dependent variable ω is specified on 400 and 700 mb levels, whereas p_s and ω_s are the values at the surface having orographic height H.

2.3. *Finite difference scheme*

The primitive equations, in flux form, are having the space differential terms of the type $\frac{\partial}{\partial x}(AB)$ and $A\frac{\partial B}{\partial x}$. The finite difference expressions adopted for space differential are derived (Okamura 1975) on the principle of conservation of total mass and energy of the system. The finite difference notations and expressions for the above two terms are :

$$D_x (A_* B)_i = \frac{1}{8d\delta_i}\left[\left\{A_{i+1}(\delta_{i+1} + \delta_i) + A_i(3\delta_i - \delta_{i+1})\right\}(B_{i+1} + B_i) - \left\{A_{i-1}(\delta_{i-1} + \delta_i) + A_i(3\delta_i - \delta_{i-1})\right\}(B_i + B_{i-1})\right] \tag{8}$$

and

$$G_x (A, B)_i = \frac{1}{4d}\left\{(A_{i+1} + A_i)(B_{i+1} - B_i) + (A_i + A_{i-1})(B_i - B_{i-1})\right\} \tag{9}$$

respectively.

Here i represents the running index in x direction. Similar notations can be used for the space differentials in y direction.

The finite difference analogue of the primitive equations and the treatment regarding the grid points which are close to orography etc are similar to that of Okamura (1976).

3. Initial fields and the specification of terrain

Initially the zonal flow $U = 10$ mps is assumed to be present without any shear in vertical as well as lateral direction. The wind and height are related by geostrophic approximation. The height field, thus, can be obtained from wind by using the expression :

$$Z_l = \bar{Z}_l - \frac{U}{g}\int_0^y f\,dy \tag{10}$$

where l varies from 1 to 3 for three different levels.

$\bar{Z}_1 = 10{,}326$ m, $\bar{Z}_2 = 4{,}848$ m and $\bar{Z}_3 = 1{,}452$ m. The sea level pressure is obtained by using the expression :

$$P_{Sea} = 1013 - \frac{1013 - 850}{\bar{Z}_3}\,\frac{U}{g}\int_0^y f\,dy \tag{11}$$

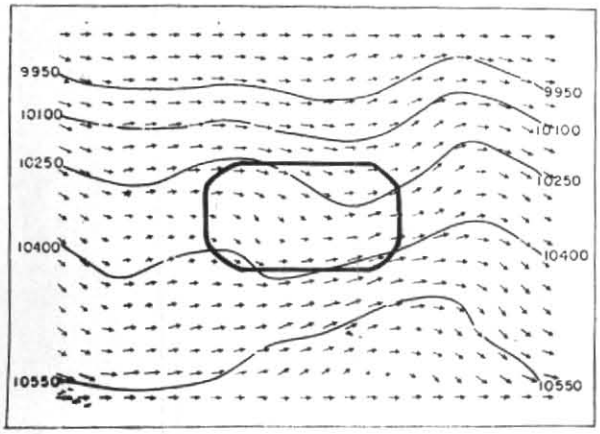

Fig. 3. Wind and height fields at 250 mb level. Forecast : 120 hours, Scale for wind speed : 1 mm=2 mps

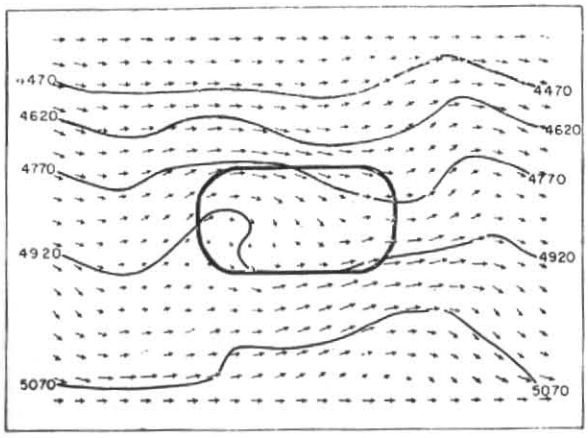

Fig. 4. Wind and height fields at 550 mb level. Forecast : 120 hours. Scale for wind speed : 1 mm=2 mps

TABLE 1

Specification of the initial values

Lat. (°N)	Heights of isobaric levels (m) Z_1	Z_2	Z_3	Temperature (°A) T_1	T_2	T_3	Sea level pressure p sea (mb)
85	9773	4295	899	249.5	270.7	281.2	951.1
80	9856	4378	982	249.5	270.7	281.2	960.5
75	9936	4458	1062	249.5	270.7	281.2	969.4
70	10011	4533	1137	249.5	270.7	281.2	977.9
65	10082	4604	1208	249.5	270.7	281.2	985.8
60	10149	4671	1275	249.5	270.7	281.2	993.4
55	10212	4734	1338	249.5	270.7	281.2	1000.5
50	10271	4793	1397	249.5	270.7	281.2	1007.1
45	10326	4848	1452	249.5	270.7	281.2	1013.2
40	10376	4896	1502	249.5	270.7	281.2	1018.9
35	10422	4944	1548	249.5	270.7	281.2	1024.1
30	10465	4987	1591	249.5	270.7	281.2	1028.8
25	10503	5025	1629	249.5	270.7	281.2	1033.1
20	10537	5059	1663	249.5	270.7	281.2	1037.1
15	10567	5089	1693	249.5	270.7	281.2	1040.3
10	10592	5114	1718	249.5	270.7	281.2	1043.2
5	10614	5136	1740	249.5	270.7	281.2	1045.6

The hydrostatic approximation is used to compute temperature T at different levels and assuming no mountains. The computed initial values are shown in Table 1.

The orographic heights are computed using the expression :

$$H = H_m\sqrt{1 - R^2} \quad \text{for } R \leqslant 1$$
$$= 0 \quad \text{for } R > 1 \qquad (12)$$

where,

$$R^2 = \frac{X^2}{R_x^2} + \frac{Y^2}{R_y^2} \qquad (13)$$

$H_m = 1000$ m, $R_x = 2000$ km and $R_y = 1000$ km

The surface pressure is now obtained by using again the hydrostatic approximation.

The computed height of the orography at various points and corresponding surface pressure are shown in Table 2.

Matsuno's (1966) time integration scheme is used for integration. The scheme has desirable effects of suppressing the high frequency gravity waves.

The model was integrated for 5 days using CDC-3600 computer without using any type of smoothing. The time step of 12-minute was used for integration.

4. Results and discussion

The forecast results are obtained for all the five days, but the results for 5th day only are presented.

4.1. *Geopotential height and wind fields*

The geopotential height and wind fields for the forecast of 120 hours are shown in Figs. 3 to 5 for 250, 550 and 850 mb levels respectively. The formation of the ridge on the windward side and the trough on the leeward side of the barrier is seen. The secondary ridge away from the barrier on the eastward side is also seen. The troughs and ridges as mentioned above are formed due to barrier effect of large orography when the westerly flows cross over it. These oscillations are introduced due to β effect.

The wind fields show reduction of the speed in central west part where the flows approach towards orography. The southeast and the northwest sectors near orography show enhancement in the wind speed.

4.2. *Surface pressure departure*

The development of high pressure on the windward side and the low pressure on the leeward side

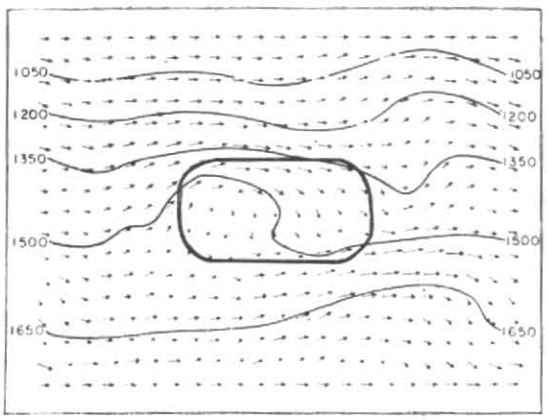

Fig. 5. Wind and height fields at 850 mb level. Forecast : 120 hours. Scale for wind speed : 1 mm = 2 mps

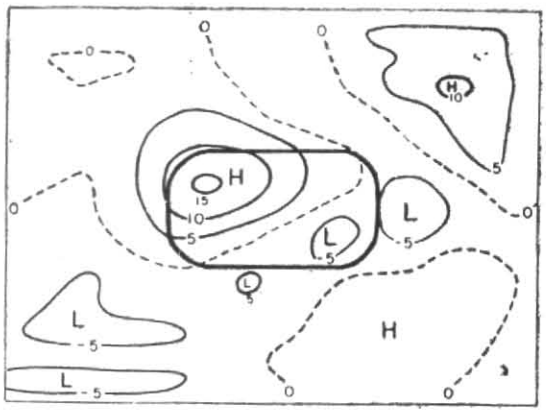

Fig. 6. Surface pressure departure $\triangle P_\theta = P_{s_{120}} - P_{s_0}$

TABLE 2

Orographic heights and corresponding surface pressure values in elliptic domain

(Unit : Orographic height in metres and surface pressure values in mb)

	440 (948.2)	630 (926.5)	720 (916.4)	750 (913.0)	720 (916.4)	630 (926.5)	440 (948.2)	
500 (948.0)	730 (921.8)	850 (908.5)	920 (900.8)	940 (998.6)	920 (900.8)	850 (908.5)	730 (921.8)	500 (948.0)
600 (942.8)	800 (920.1)	920 (906.8)	980 (900.2)	1000* (898.0)	980 (900.2)	920 (906.8)	800 (920.1)	600 (942.8)
500 (960.3)	730 (933.7)	850 (920.2)	920 (912.4)	940 (910.2)	920 (912.4)	850 (920.2)	730 (933.7)	500 (960.3)
	440 (972.8)	630 (950.5)	720 (940.2)	750 (936.7)	720 (940.2)	630 (950.5)	440 (972.8)	

NOTE : Bracketed figures are surface pressure values in mb.

*Centre of region with H_m = (1000 metres).

of the orography and also the secondary high pressure development towards eastern side of the fully developed flow are observed (*see* Fig. 6).

Initial development in 12 hours forecast indicates development of high pressure on the windward side (+ 4.9 mb) and symmetrical low pressure departure on leeward side (− 4.4 mb). The zero isopleth is almost in the direction of the y axis thro' the centre of the orography. Similarly the 2nd isopleth of zero line is towards eastern side more or less parallel to the first isoline. Subsequent forecasts show rapid development especially in the leeward trough and the ridge.

4.3. *Vertical p-velocity and thermal changes*

The vertical velocity fields for 400 and 700 mb and the surface are shown in Figs. 7, 8 and 9 respectively. The vertical velocity is upward on the windward side of the mountain and is downward on the lee side. The magnitude of the vertical velocity, in general, is maximum at the surface and decreases aloft. The upward vertical velocity on the windward side of the mountain is due to forced ascent of the flow whereas the downward vertical velocity on the leeward side is due to descending of the flows along the downslopes of the barrier. The vertical velocity is also upward on the eastward side away from the orography at 400 and 700 mb levels. This may be due to 'Rossby' type of oscillation and associated vertical velocity on the leeward side.

The temperature changes at 700 mb level are shown in Fig. 10. The temperature departures are negative on the windward side and positive on the leeward side of the barrier indicating cooling and warming respectively. The cooling and warming as mentioned above are appropriate in view of the upward and downward vertical velocities developed respectively in these regions. The cooling and warming can be explained to certain extent on the basis of dry adiabatic cooling or warming observed when the parcel of air is displaced vertically upward or downward respectively. The actual cooling or warming in the model atmosphere, however, is difficult to estimate as the flow is constantly getting evolved. The temperature is also changed due to horizontal advection.

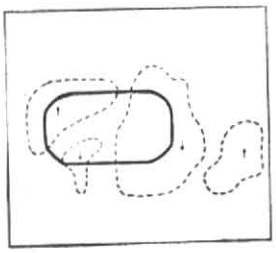

Fig. 7. Vertical velocity ω at 120 hrs, level : 400 mb. Unit : 10^{-3}mb sec^{-1}. (Contour spacing is at 0.3 unit interval)

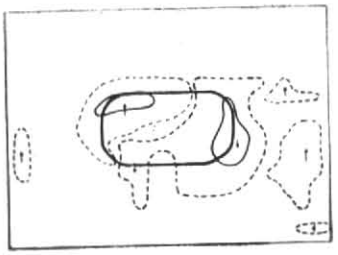

Fig. 8. Vertical velocity ω at 120 hrs. Level : 700 mb. Unit : 10^{-3} mb sec^{-1} (Contour spacing is at 0.3 unit interval)

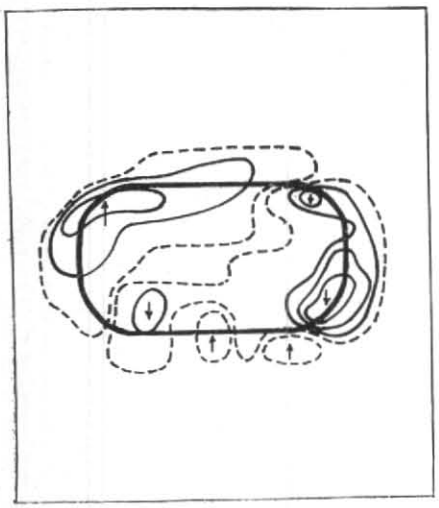

Fig. 9. Vertical velocity ω_s at 120 hrs. Level : Surface, Unit : 10^{-3} mb sec^{-1}. (Contour spacing is at 0.3 unit interval)

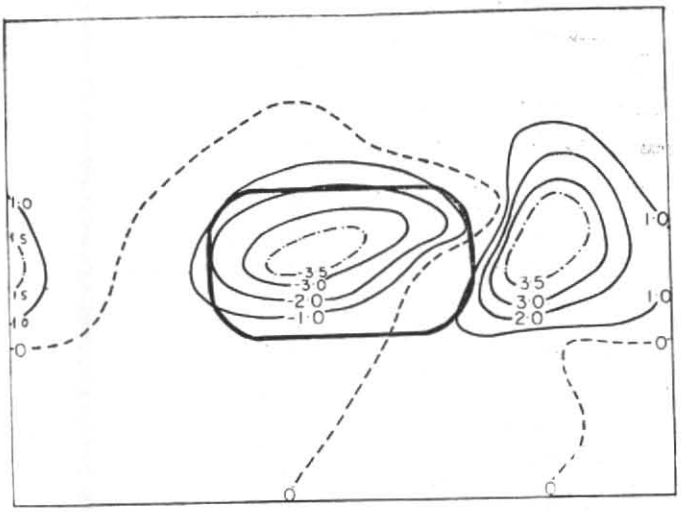

Fig. 10. Temperature departure $\Delta T = T_{120} - T_0$ (°C) Level : 700 mb

5. Concluding remarks

This experiment is performed without the inclusion of frictional and diffusion terms in the momentum and thermal equations. The effect of these terms on forecast fields will be studied in the separate experiment.

The present experiment shows the proper simulation of the dynamic effects of low type of orographic barrier. The conspicuous features are: (1) Development of upstream ridge and upward vertical velocity due to forced ascent. The corresponding temperature changes are negative indicating cooling, (2) Development of downstream trough and downward vertical velocity and the associated positive temperature departure indicating heating and (3) The development of the ridge on the eastward side away from the orography.

The formation of the troughs and ridges as mentioned is due to β effect when the westerly flow is perturbed due to large scale orographic forcing. The trough on the western side of the domain of integration is also seen but this may be due to artificiality of the cyclic boundary conditions imposed at the eastern and western boundaries of the limited area model at every time-step with the cycle of length *'L'* (*see* Fig. 1).

Acknowledgement

The authors' grateful thanks are due to Dr. Bh. V. Ramana Murty and Dr. D. A. Mooley for the interest in this work. Thanks are also due to Shri D. R. Sikka

and Shri S. K. Mishra for the useful discussions with them and to Mrs. Sathy Nair for typing the manuscript.

List of symbols

u	Wind component in x direction; positive towards east.
v	Wind component in y direction; positive towards north.
ω	The vertical p velocity.
f	Coriolis parameter.
ϕ	Geopotential height.
F_x, F_y	Frictional and diffusion terms in u and v momentum equations respectively.
D_t	Diffusion term in thermal equation.
R	Specific gas constant.
T	Temperature in °A.
c_p	Specific heat at constant pressure.
β	The variation of coriolis parameter in y direction.
p_s	Surface pressure.
P_{sea}	Sea level pressure.
u_s, v_s	Wind components at surface in x, y directions
ω_s	Vertical p velocity at surface.
A, B	Arbitrary variables
δ_i	Pressure interval of the layer at ith point.
Z	Height of the isobaric surface.
$\bar{Z}$	Mean height.
U	Constant wind.
H	Orographic height.
H_m	Maximum height of the orography at the centre of the region.
R_x	The maximum distance (from the centre) of orography in x direction.
R_y	The maximum distance (from the centre) of orography in y direction
R	The horizontal distance between the point on elliptic orography and its centre.
d	Grid length = 5°.

References

Das, P.K. and Bedi, H.S., 1976, 'A study on orographic effects by a primitive equation model', Proc. symp. on Tropical Monsoon IITM, pp. 51–58.

Matsuno, T., 1966, 'Numerical integration of the primitive equations by a simulated backward difference method. *J. met. Soc. Japan*, **44**, pp. 76–84.

Okamura, Y., 1975, 'Computational design of a limited area prediction model, *J. met. Soc. Japan*, **53**, pp. 175–188.

Okamura, Y., 1976, 'Numerical experiments of orographic effect on the large scale motion of the atmosphere, *Pap. Met. Geophys.*, **27**, pp. 1–20.

Singh, S.S. and Saha, K.R., 1976, 'Preliminary results of integration of a five-layer primitive equation model, Proc. Symp. on Tropical Monsoons, IITM, pp. 43–50.